Computer Aided Geometric Design 88 (2021) 102003

Contents lists available at ScienceDirect

Computer Aided Geometric Design

www.elsevier.com/locate/cagd

New shape control tools for rational Bézier curve design

Andriamahenina Ramanantoanina, Kai Hormann *

Università della Svizzera italiana, Lugano, Switzerland

ARTICLE INFO

Article history:
Available online 20 May 2021

Keywords:
Rational Bézier curve
Barycentric rational interpolation
Curve design

ABSTRACT

Bézier curves are indispensable for geometric modelling and computer graphics. They have numerous favourable properties and provide the user with intuitive tools for editing the shape of a parametric polynomial curve. Even more control and flexibility can be achieved by associating a shape parameter with each control point and considering rational Bézier curves, which comes with the additional advantage of being able to represent all conic sections exactly. In this paper, we explore the editing possibilities that arise from expressing a rational Bézier curve in barycentric form. In particular, we show how to convert back and forth between the Bézier and the barycentric form, we discuss the effects of modifying the constituents (nodes, interpolation points, weights) of the barycentric form, and we study the connection between point insertion in the barycentric form with degree elevation of the Bézier form. Moreover, we analyse the favourable performance of the barycentric form for evaluating the curve.

1. Introduction

A planar *rational Bézier curve* $P\colon [0,1] \to \mathbb{R}^2$ of *degree* $n \in \mathbb{N}$ is defined by a set of *control points* $P_0, \dots, P_n \in \mathbb{R}^2$ and a set of *weights* $\alpha_0, \dots, \alpha_n \in \mathbb{R}$ as

$$P(t) = \big(x(t), y(t)\big) = \frac{\sum_{i=0}^{n} \alpha_i B_i^n(t) P_i}{\sum_{i=0}^{n} \alpha_i B_i^n(t)}, \tag{1}$$

where $B_i^n(t) = \binom{n}{i}(1-t)^{n-i}t^i$ are the Bernstein polynomials. If $\alpha_0 = \alpha_n = 1$, then the curve is said to be in *standard form*, which can always be achieved, if the given weights α_0 and α_n are non-zero and have the same sign, by uniformly scaling all weights and applying a linear rational parameter transformation (Patterson, 1985; Farin and Worsey, 1991). The curve P can also be written in homogeneous form and understood as the (central) projection of the spatial polynomial Bézier curve $\hat{P}\colon [0,1] \to \mathbb{R}^3$,

$$\hat{P}(t) = \big(\hat{x}(t), \hat{y}(t), \hat{z}(t)\big) = \sum_{i=0}^{n} B_i^n(t) \hat{P}_i, \tag{2}$$

with homogeneous control points $\hat{P}_i = (\alpha_i P_i, \alpha_i) \in \mathbb{R}^3$ into the $\hat{z} = 1$ plane, because $x(t) = \hat{x}(t)/\hat{z}(t)$ and $y(t) = \hat{y}(t)/\hat{z}(t)$. If all weights α_i are equal, then P reduces to a planar polynomial Bézier curve.

* Corresponding author.
E-mail addresses: andriamahenina.ramanantoanina@usi.ch (A. Ramanantoanina), kai.hormann@usi.ch (K. Hormann).

https://doi.org/10.1016/j.cagd.2021.102003
0167-8396/

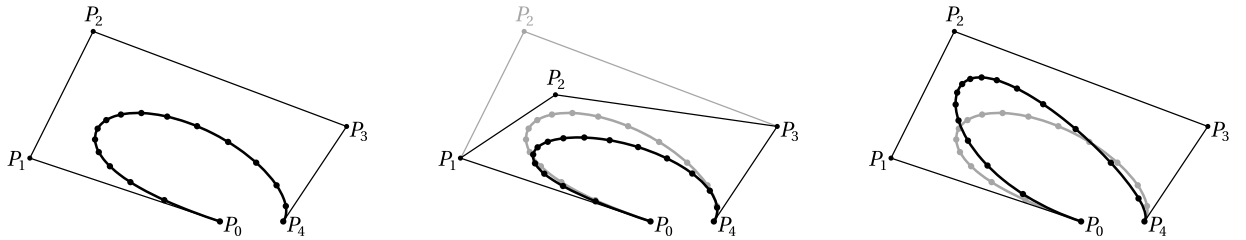

Fig. 1. (a) A rational Bézier curve of degree $n = 4$ with weights $\alpha = (1, 3/2, 1, 1/2, 1)$; (b) the effect of moving the control point P_2; (c) the effect of increasing the weight α_2 from 1 to 3. The dots visualize the curve points $P(i/16)$ for $i = 0, \dots, 16$.

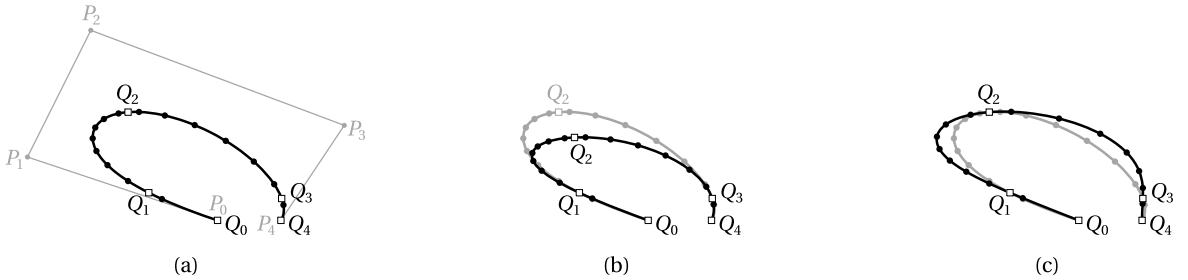

Fig. 2. (a) Converting a rational Bézier curve in (1) to the barycentric form in (3); (b) the effect of moving the interpolation point Q_2; (c) the effect of decreasing the weight β_2 by 50%. The dots visualize the curve points $P(i/16)$ for $i = 0, \dots, 16$.

Among the key properties that justify the popularity of rational Bézier curves for shape design, we recall that such a curve can be translated, scaled, or rotated by simply translating, scaling, or rotating its control polygon, and the same holds more generally for projective transformations (Farin, 2001). Moreover, the shape of the curve can be controlled intuitively by modifying the control points P_i and the weights α_i (see Fig. 1), or by changing the *Farin points* $F_i = (\alpha_i P_i + \alpha_{i+1} P_{i+1})/(\alpha_i + \alpha_{i+1}) \in \mathbb{R}^2$ that can be associated with the i-th edge $[P_i, P_{i+1}]$ of the control polygon for $i = 0, \dots, n-1$ (Farin, 1983). However, except at the endpoints, this control is *indirect* in the sense that it is difficult for the user to let the curve pass *exactly* through a specific point $Q \in \mathbb{R}^2$.

To overcome this limitation, we propose to convert the curve P to *barycentric form* and express it as

$$P(t) = \frac{\sum_{i=0}^{n} (-1)^i \frac{\beta_i}{t - t_i} Q_i}{\sum_{i=0}^{n} (-1)^i \frac{\beta_i}{t - t_i}}, \tag{3}$$

for certain distinct *nodes* $t_0, \dots, t_n \in \mathbb{R}$ with corresponding *interpolation points* $Q_0, \dots, Q_n \in \mathbb{R}^2$ and non-zero *weights* $\beta_0, \dots, \beta_n \in \mathbb{R}$. Since $P(t_i) = Q_i$, by construction (Schneider and Werner, 1986), this representation allows for *direct* control, as we can force the curve to pass through some $Q \in \mathbb{R}^2$ by simply moving one of the Q_i to Q. Moreover, the "flatness" of the curve at Q_i can be controlled by modifying the weight β_i (see Fig. 2).

To the best of our knowledge, the barycentric form has been studied only in the functional setting, so far. For polynomials, it can be traced back to Taylor (1945) and Dupuy (1948), and Berrut and Trefethen (2004) provide a detailed summary of its favourable properties. For rational functions, Salzer (1981) and Schneider and Werner (1986) were the first to identify the advantages of the barycentric form, and Berrut and Mittelmann (1997) show that every rational interpolant can be expressed in barycentric form for a suitable choice of weights. For very specific weights, barycentric rational interpolants are guaranteed to have no poles and a high approximation order (Berrut, 1988; Floater and Hormann, 2007), with slow-growing Lebesgue constants, in particular for equidistant nodes (Bos et al., 2012). The barycentric form is also a key ingredient of the AAA algorithm (Nakatsukasa et al., 2018), which extends the work of Antoulas and Anderson (1986) and uses an adaptive node selection scheme for efficiently computing robust rational approximations of real and complex functions.

1.1. Contributions

In contrast to this previous work, the aim of this paper is to explore the use of the barycentric form in the context of curve design. We first show that rational Bézier curves (1) and barycentric rational curves (3) are essentially equivalent (Section 2), in the sense that any rational Bézier curve can be expressed in barycentric form and vice versa. We then discuss the shape editing possibilities offered by the barycentric form (Section 3), we show how to raise the degree from n to $n+1$ without changing the curve (Section 4), and provide numerical evidence that the barycentric form is advantageous for curve evaluation (Section 5).

2. Equivalence of Bézier and barycentric form

Let us first recall how to derive the barycentric form for a polynomial $p\colon \mathbb{R} \to \mathbb{R}$ of degree n (Berrut and Trefethen, 2004). Clearly, the Lagrange form of p is

$$p(t) = \sum_{i=0}^{n} \prod_{j=0,\, j\neq i}^{n} \frac{t-t_j}{t_i-t_j} p_i$$

where $p_i = p(t_i)$, $i = 0, \dots, n$. Factoring out the polynomial $\ell(t) = \prod_{j=0}^{n}(t-t_j)$, we get the *first barycentric form*

$$p(t) = \ell(t) \sum_{i=0}^{n} \frac{w_i}{t-t_i} p_i,$$

with the *Lagrange weights* w_i defined as

$$w_i = \prod_{j=0,\, j\neq i}^{n} \frac{1}{t_i-t_j}, \qquad i = 0, \dots, n. \tag{4}$$

Further dividing by the constant function 1, expressed in first barycentric form as $1 = \ell(t) \sum_{i=0}^{n} \frac{w_i}{t-t_i}$, and cancelling the common factor $\ell(t)$, then yields the *second barycentric form*

$$p(t) = \frac{\sum_{i=0}^{n} \frac{w_i}{t-t_i} p_i}{\sum_{i=0}^{n} \frac{w_i}{t-t_i}}.$$

To convert the rational Bézier curve in (1) to the barycentric form in (3), it remains to express the two components $\hat{x}(t)$, $\hat{y}(t)$ in the numerator of $P(t)$ and its denominator $\hat{z}(t)$ in the first barycentric form.

Proposition 1. *For any nodes $0 \le t_0 < t_1 < \cdots < t_n \le 1$, we can express the rational Bézier curve (1) with control points P_i and weights α_i in barycentric form (3) with interpolation points $Q_i = P(t_i)$ and weights $\beta_i = (-1)^{n+i} w_i z_i$, where $z_i = \hat{z}(t_i)$ and w_i as in (4).*

Proof. Let us first write the denominator of $P(t)$ in first barycentric form as

$$\hat{z}(t) = \sum_{i=0}^{n} \alpha_i B_i^n(t) = \ell(t) \sum_{i=0}^{n} \frac{w_i}{t-t_i} z_i. \tag{5}$$

Likewise, the numerator of $P(t)$ can be expressed in first barycentric form as

$$\sum_{i=0}^{n} \alpha_i B_i^n(t) P_i = \hat{z}(t) P(t) = \ell(t) \sum_{i=0}^{n} \frac{w_i}{t-t_i} z_i P(t_i). \tag{6}$$

The statement then follows after dividing (6) by (5), substituting $P(t_i) = Q_i$ and $w_i z_i = (-1)^{n+i}\beta_i$, and cancelling the common factor $(-1)^n \ell(t)$. □

In principle, the nodes t_i do not have to be ordered or restricted to the interval $[0, 1]$, as long as they are distinct; however, in the context of interactive curve design, it seems natural to make these assumptions. Likewise, it is reasonable to set $t_0 = 0$ and $t_n = 1$, so that $Q_0 = P_0$ and $Q_n = P_n$ mark the endpoints of the curve.

Under the usual assumption of positive weights α_i, which guarantees that $\hat{z}(t) > 0$ for all $t \in [0, 1]$, so that the curve is non-singular,[1] we conclude that the weights β_i are positive, too, because $\operatorname{sign}(w_i) = (-1)^{n-i}$, which follows from the observation that the factors of w_i in (4) are negative, if and only if $i < j \le n$. This is in line with a result by Schneider and Werner (1986, Proposition 8), which implies that the positivity of the β_i is a necessary condition for the non-singularity of the barycentric rational curve in (3).

Example 1. Consider the quadratic rational curve P in Bézier form (1) with control points $P_0 = (1, 0)$, $P_1 = (1, 1)$, $P_2 = (0, 1)$ and weights $\alpha_0 = 1$, $\alpha_1 = 1/\sqrt{2}$, $\alpha_2 = 1$, which describes a quarter circle (see Fig. 3.a). Sampling this curve at the nodes $t_0 = 0$, $t_1 = 2 - \sqrt{2}$, $t_2 = 1$ yields the interpolation points $Q_0 = (1, 0)$, $Q_1 = (3/5, 4/5)$, $Q_2 = (0, 1)$, and the weights of the barycentric form (3) turn out to be $\beta_0 = 1 + 1/\sqrt{2}$, $\beta_1 = 5/\sqrt{2}$, $\beta_2 = 1 + \sqrt{2}$ (see Fig. 3.b).

[1] It is actually sufficient to assume $\alpha_0, \alpha_n > 0$ and $\alpha_i \ge 0$ for $i = 1, \dots, n-1$.

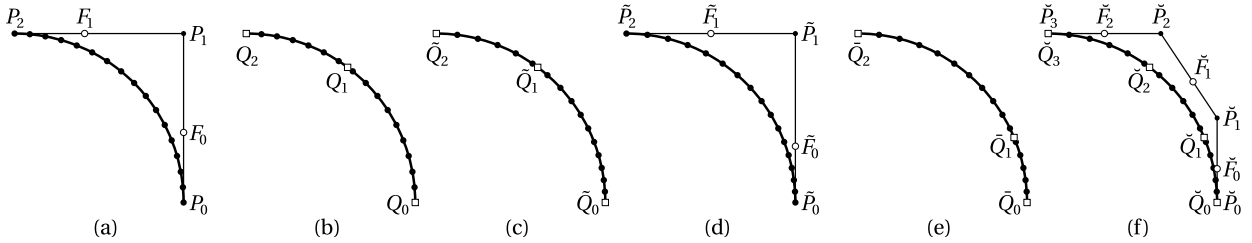

Fig. 3. Different representations of the quarter circle as a quadratic rational curve: (a) standard Bézier form with $\alpha_0 = \alpha_2 = 1$ (instead of the weights α_i we show the Farin points F_i to visualize the ratios α_i/α_{i+1}); (b) corresponding barycentric form (cf. Proposition 1) for $t_0 = 0$, $t_1 = 2 - \sqrt{2}$, $t_2 = 1$; (c) standard barycentric form with $\tilde{\beta}_0 = \tilde{\beta}_2 = 1$ after reparameterization (cf. Proposition 3); (d) corresponding (non-symmetric) Bézier form (cf. Proposition 4); (e) after sliding the interpolation point $\tilde{Q}_1$ to the new position $\bar{Q}_1$ (cf. Proposition 5); (f) as a cubic rational curve after inserting an additional interpolation point (cf. Proposition 7), in barycentric and Bézier form. The dots visualize the curve points $P(i/16)$ for $i = 0, \dots, 16$.

Once a rational curve is represented in barycentric form, we can use a linear rational reparameterization to bring it into *standard barycentric form* with $\beta_0 = \beta_n = 1$, very similarly to how the Bézier representation can be brought into standard form (Patterson, 1985).

Lemma 2. *For any $\lambda \in (0, 1)$, consider the linear rational reparameterization $\varphi\colon [0, 1] \to [0, 1]$,*

$$\varphi(t) = \frac{(1-\lambda)t}{\lambda(1-t) + (1-\lambda)t}. \tag{7}$$

Let P be the barycentric rational curve (3) with nodes t_i, interpolation points Q_i, and weights β_i and let $\tilde{P}$ be the barycentric rational curve with nodes $\tilde{t}_i = \varphi(t_i)$, the same interpolation points $\tilde{Q}_i = Q_i$, and weights $\tilde{\beta}_i = \beta_i \lambda \tilde{t}_i / t_i$. Then, $P = \tilde{P} \circ \varphi$.

Proof. Denoting the denominator of $\varphi(t)$ by $\delta(t) = \lambda(1-t) + (1-\lambda)t$, we first observe that

$$\frac{\tilde{t}_i}{\varphi(t) - \tilde{t}_i} = \frac{\varphi(t_i)}{\varphi(t) - \varphi(t_i)} = \frac{\frac{(1-\lambda)t_i}{\delta(t_i)}}{\frac{(1-\lambda)t}{\delta(t)} - \frac{(1-\lambda)t_i}{\delta(t_i)}} = \frac{t_i \delta(t)}{t\delta(t_i) - t_i\delta(t)} = \frac{t_i \delta(t)}{\lambda(t - t_i)}$$

for any $i = 0, \dots, n$. Therefore,

$$\frac{\tilde{\beta}_i}{\varphi(t) - \tilde{t}_i} = \frac{\beta_i \lambda}{t_i} \cdot \frac{\tilde{t}_i}{\varphi(t) - \tilde{t}_i} = \frac{\beta_i}{t - t_i} \delta(t).$$

After substituting this into the numerator and the denominator of $(\tilde{P} \circ \varphi)(t)$ and cancelling the common factor $\delta(t)$ we get $(\tilde{P} \circ \varphi)(t) = P(t)$. □

Note that $\tilde{\beta}_0$ in Lemma 2 is well-defined, even if $t_0 = 0$, because

$$\lim_{t \to 0} \frac{\varphi(t)}{t} = \lim_{t \to 0} \varphi'(t) = \frac{1-\lambda}{\lambda},$$

so that $\tilde{\beta}_0 = \beta_0(1-\lambda)$ in that case. Moreover, we observe that $\operatorname{sign}(\tilde{\beta}_i) = \operatorname{sign}(\beta_i)$ for $i = 0, \dots, n$. Therefore, if the β_i are all positive, then so are the new weights $\tilde{\beta}_i$.

Proposition 3. *The barycentric rational curve (3) with nodes t_i, interpolation points Q_i, and weights β_i can be expressed in standard form by first reparameterizing it with φ in (7) for*

$$\lambda = \frac{\beta_0 t_n - \beta_n t_0}{\beta_0(2t_n - 1) - \beta_n(2t_0 - 1)} \tag{8}$$

and then dividing all weights $\tilde{\beta}_i$ by $\tilde{\beta}_0$, as long as $\lambda \in (0, 1)$.

Proof. According to Lemma 2, the first and the last weight of the reparameterized curve are

$$\tilde{\beta}_0 = \beta_0 \lambda \frac{\varphi(t_0)}{t_0} = \frac{\beta_0}{\delta(t_0)} \lambda(1-\lambda) \qquad \text{and} \qquad \tilde{\beta}_n = \beta_n \lambda \frac{\varphi(t_n)}{t_n} = \frac{\beta_n}{\delta(t_n)} \lambda(1-\lambda), \tag{9}$$

where $\delta(t)$ is again the denominator of $\varphi(t)$. It remains for us to show that the choice of λ in (8) guarantees $\tilde{\beta}_0 = \tilde{\beta}_n$, which is equivalent to $\beta_0 \delta(t_n) = \beta_n \delta(t_0)$ by (9), so that both weights are 1 after dividing them by $\tilde{\beta}_0$. But as (8) implies

$$\lambda\beta_0(2t_n - 1) - \lambda\beta_n(2t_0 - 1) = \beta_0 t_n - \beta_n t_0$$

and further

$$\beta_n t_0 - 2\lambda\beta_n t_0 + \lambda\beta_n = \beta_0 t_n - 2\lambda\beta_0 t_n + \lambda\beta_0,$$

we get the desired identity after noting that $\delta(t_0) = \lambda - 2\lambda t_0 + t_0$ and $\delta(t_n) = \lambda - 2\lambda t_n + t_n$. □

The curve cannot be brought into standard form, if λ in (8) is outside the open interval $(0, 1)$, because φ is singular and no longer a monotonic reparameterization of $[0, 1]$ in that case. However, if $t_0 = 0$, $t_n = 1$, and all β_i are positive, then λ simplifies to $\lambda = \beta_0/(\beta_0 + \beta_n) \in (0, 1)$ and $\tilde{\beta}_0 = \tilde{\beta}_n = \beta_0\beta_n/(\beta_0 + \beta_n) > 0$.

Example 2. Applying Proposition 3 to the barycentric rational curve P from Example 1 (see Fig. 3.b), it turns out that the quarter circle can be described in standard barycentric form with nodes $\tilde{t}_0 = 0$, $\tilde{t}_1 = 2/3$, $\tilde{t}_2 = 1$, interpolation points $\tilde{Q}_0 = (1, 0)$, $\tilde{Q}_1 = (3/5, 4/5)$, $\tilde{Q}_2 = (0, 1)$, and weights $\tilde{\beta}_0 = 1$, $\tilde{\beta}_1 = 5/3$, $\tilde{\beta}_2 = 1$ (see Fig. 3.c).

A natural question to ask at this point is: how does one get back from barycentric to Bézier form? To this end, it helps to recall that $\hat{P}_i = (\alpha_i P_i, \alpha_i)$ and to let $\hat{Q}_i = (z_i Q_i, z_i)$, so that the assignments $Q_i = P(t_i)$ and $z_i = \hat{z}(t_i)$ for $i = 0, \dots, n$ in the statement of Proposition 1 can be written compactly as $\hat{\boldsymbol{Q}} = \boldsymbol{B}\hat{\boldsymbol{P}}$, where[2]

$$\boldsymbol{B} = \begin{pmatrix} B_0^n(t_0) & \cdots & B_n^n(t_0) \\ \vdots & \ddots & \vdots \\ B_0^n(t_n) & \cdots & B_n^n(t_n) \end{pmatrix}, \qquad \hat{\boldsymbol{P}} = \begin{pmatrix} \hat{P}_0 \\ \vdots \\ \hat{P}_n \end{pmatrix}, \qquad \hat{\boldsymbol{Q}} = \begin{pmatrix} \hat{Q}_0 \\ \vdots \\ \hat{Q}_n \end{pmatrix}. \tag{10}$$

Proposition 4. *The barycentric rational curve (3) with nodes t_i, interpolation points Q_i, and weights β_i can be expressed in Bézier form (1) with control points $P_i = (\hat{x}_i, \hat{y}_i)/\hat{z}_i$ and weights $\alpha_i = \hat{z}_i$, where the vector $\hat{\boldsymbol{P}}$ of points $\hat{P}_i = (\alpha_i P_i, \alpha_i) = (\hat{x}_i, \hat{y}_i, \hat{z}_i)$ is defined as $\hat{\boldsymbol{P}} = \boldsymbol{B}^{-1}\hat{\boldsymbol{Q}}$ and $\hat{\boldsymbol{Q}}$ is the vector of points $\hat{Q}_i = (z_i Q_i, z_i)$ with $z_i = (-1)^{n+i}\beta_i/w_i$ and w_i as in (4).*

Proof. First recall that the *Bernstein–Vandermonde* matrix $\boldsymbol{B}$ in (10) is non-singular, because the Bernstein basis is a Chebyshev system. The assertion then follows immediately by applying Proposition 1 to the rational Bézier curve with the stated control points P_i and weights α_i and verifying that it gives back the interpolation points Q_i and weights β_i. □

Note that $\hat{\boldsymbol{P}} = \boldsymbol{B}^{-1}\hat{\boldsymbol{Q}}$ can be computed fast and accurately with $O(n^2)$ time complexity (Marco and Martínez, 2007). If the last coordinate $\alpha_i = \hat{z}_i$ of the homogeneous control point $\hat{P}_i$ happens to vanish for some i, it means that the given barycentric rational curve cannot be written as a classical rational Bézier curve with control points in $\mathbb{R}^2$. Instead, the control point P_i needs to be replaced by the *control vector* $\alpha_i P_i = (\hat{x}_i, \hat{y}_i) \in \mathbb{R}^2$, representing an *infinite* control point in this case (Piegl, 1987; Farin, 2001).

Example 3. Using Proposition 4 to convert the barycentric rational curve $\tilde{P}$ in standard form from Example 2 (see Fig. 3.c) back to Bézier form, we find that the quadratic rational Bézier curve with control points $\tilde{P}_0 = (1, 0)$, $\tilde{P}_1 = (1, 1)$, $\tilde{P}_2 = (0, 1)$ and weights $\tilde{\alpha}_0 = 2/3$, $\tilde{\alpha}_1 = 1/3$, $\tilde{\alpha}_2 = 1/3$ also describes a quarter circle (see Fig. 3.d). Bringing these weights into standard form, we return to the rational Bézier curve P that we started with in Example 1 (see Fig. 3.a).

3. Shape editing using the barycentric form

Once a rational curve is given in barycentric form (3), several new options arise for manipulating the curve by modifying the different parameters of the barycentric form: the nodes t_i, the interpolation points Q_i, and the weights β_i.

Changing one of the nodes, say t_k, in isolation, while keeping the Q_i and the β_i fixed, has a rather unpredictable effect. However, it is possible to preserve the shape (and the parameterization) of the curve by simultaneously adapting the corresponding Q_k and all β_i, so that the effect amounts to "sliding" Q_k along the curve. This can be achieved by first using Proposition 4 to express the curve in Bézier form and then applying Proposition 1 with the modified nodes to get back to the barycentric form. However, it turns out that we do not have to carry out these conversions explicitly, as the new interpolation points and weights can be expressed directly in terms of the given parameters of the barycentric form.

Proposition 5. *Suppose we change the node t_k for some $k \in \{0, \dots, n\}$ to some new value $\bar{t}_k \notin \{t_0, \dots, t_n\}$ and keep the other nodes fixed, that is, we let $\bar{t}_i = t_i$ for $i \neq k$. The barycentric rational curve (3) with nodes t_i, interpolation points Q_i, and weights β_i can then be expressed alternatively in terms of the nodes $\bar{t}_i$, the interpolation points $\bar{Q}_k = P(\bar{t}_k)$ and $\bar{Q}_i = Q_i$ for $i \neq k$, and the weights*

[2] The observant reader may have already noticed that throughout this paper we write *points* (in $\mathbb{R}^2$ and $\mathbb{R}^3$) as *row vectors*, so as to avoid excessive use of the transposition operator and to be able to conveniently stack them into matrices, like $\hat{\boldsymbol{P}}$, $\hat{\boldsymbol{Q}} \in \mathbb{R}^{(n+1)\times 3}$.

$$\bar{\beta}_k = \sum_{i=0}^{n} (-1)^{n+k+i} \frac{\bar{t}_k - t_k}{\bar{t}_k - t_i} \beta_i, \qquad \bar{\beta}_i = \frac{t_i - t_k}{t_i - \bar{t}_k} \beta_i, \quad i \neq k. \tag{11}$$

Proof. To prove this statement, we stick to the idea sketched out above. After converting the given curve to Bézier form, it follows directly from Proposition 1 that the new interpolation points are $\bar{Q}_i = P(\bar{t}_i)$, which simplifies to $\bar{Q}_i = P(t_i) = Q_i$ for $i \neq k$. Moreover, we know that the given weights satisfy $\beta_i = (-1)^{n+i} w_i \hat{z}(t_i)$, where w_i is defined in (4) and the denominator polynomial $\hat{z}$ can be written, independently of the Bézier form, in first barycentric form as $\hat{z}(t) = \ell(t) \sum_{i=0}^{n} (-1)^i \frac{\beta_i}{t - t_i}$. Likewise, the new weights satisfy $\bar{\beta}_i = (-1)^{n+i} \bar{w}_i \hat{z}(\bar{t}_i)$, where $\bar{w}_i = \prod_{j=0,\, j\neq i}^{n} \frac{1}{\bar{t}_i - \bar{t}_j}$. If $i \neq k$, then this expression simplifies to

$$\bar{\beta}_i = (-1)^{n+i} \frac{1}{\bar{t}_i - \bar{t}_k} \prod_{j=0,\, j\neq i,k}^{n} \frac{1}{\bar{t}_i - \bar{t}_j} \hat{z}(\bar{t}_i) = (-1)^{n+i} \frac{1}{t_i - \bar{t}_k} \prod_{j=0,\, j\neq i,k}^{n} \frac{1}{t_i - t_j} \hat{z}(t_i) = \frac{t_i - t_k}{t_i - \bar{t}_k} \beta_i,$$

because $\bar{t}_i = t_i$ for $i \neq k$. For the remaining weight $\bar{\beta}_k$, note that $\ell(\bar{t}_k) = \prod_{j=0}^{n} (\bar{t}_k - t_j) = (\bar{t}_k - t_k)/\bar{w}_k$, hence

$$\bar{\beta}_k = (-1)^{n+k} \bar{w}_k \ell(\bar{t}_k) \sum_{i=0}^{n} (-1)^i \frac{\beta_i}{\bar{t}_k - t_i} = \sum_{i=0}^{n} (-1)^{n+k+i} \frac{\bar{t}_k - t_k}{\bar{t}_k - t_i} \beta_i. \quad \square$$

In an interactive application, this "sliding" of Q_k can be realized, for example, by letting the user click on the desired interpolation point, while holding the 'shift' key (to distinguish the action from a displacement of Q_k; see below), and translating the subsequent mouse movement (left/right or up/down) into an increase or decrease of t_k until the mouse button is released. Note that the time complexity for updating β_k is $O(n)$, $O(1)$ for updating each of the other β_i, and $O(n)$ for updating Q_k (see Section 5), hence $O(n)$ overall, which is much more efficient than computing the conversion to Bézier form and back.

For the reasons pointed out in Section 2, it seems reasonable to prevent sliding the endpoints Q_0 and Q_n, that is, to exclude the cases $k = 0$ and $k = n$ in Proposition 5, and to restrict $\bar{t}_k$ to the open interval (t_{k-1}, t_{k+1}), so that $\bar{Q}_k$ remains between its neighbours Q_{k-1} and Q_{k+1} along the curve. In this case, it follows immediately from (11) that $\operatorname{sign}(\bar{\beta}_i) = \operatorname{sign}(\beta_i)$ for $i \neq k$, hence the positivity of the weights β_i carries over to the new weights $\bar{\beta}_i$. For $\bar{\beta}_k$, this is not obvious from (11), but implied by the fact that changing t_k does not change the curve, so that the non-singularity of the curve still guarantees that all β_i have the same weight (Schneider and Werner, 1986).

Example 4. Applying Proposition 5 to the barycentric rational curve $\tilde{P}$ in standard form from Example 2 (see Fig. 3.c) and changing $\tilde{t}_1 = 2/3$ to $\bar{t}_1 = 1/3$, thus sliding $\tilde{Q}_1 = (3/5, 4/5)$ to $\bar{Q}_1 = (12/13, 5/13)$, we find that the quarter circle can also be described in barycentric form with nodes $\bar{t}_0 = 0$, $\bar{t}_1 = 1/3$, $\bar{t}_2 = 1$, interpolation points $\bar{Q}_0 = (1, 0)$, $\bar{Q}_1 = (12/13, 5/13)$, $\bar{Q}_2 = (0, 1)$, and weights $\bar{\beta}_0 = 2$, $\bar{\beta}_1 = 13/6$, $\bar{\beta}_2 = 1/2$ (see Fig. 3.e).

The most direct control over the shape of the curve is given by displacing one of the interpolation points, say Q_k, while keeping all other parameters fixed. By the interpolation property of the barycentric form, this will force the curve to pass through the new position of Q_k at t_k (see Fig. 2.b). Compared to moving a Bézier control point P_k, it should be noted that the basis function $C_k(t) = (-1)^k \frac{\beta_k}{t - t_k} \Big/ \sum_{i=0}^{n} (-1)^i \frac{\beta_i}{t - t_i}$ that corresponds to Q_k (see Fig. 4.a) is neither non-negative nor as nicely "bell-shaped" as the basis function $\alpha_k B_k^n(t) \Big/ \sum_{i=0}^{n} \alpha_i B_i^n(t)$ that corresponds to P_k. Hence, for large displacements, the shape may change less intuitively as it does in the case of editing the control polygon. However, while the general shape of the curve is more easily controlled with the Bézier control points P_i, changing the interpolation points Q_i, combined with the "sliding" procedure outlined above and inserting points with ease (see Section 4) provides a useful tool for "micro-editing" the curve shape. For example, it can be used to "snap" the curve to some point Q that must be interpolated exactly and the interpolation property guarantees that Q remains a point on the curve during subsequent editing operations, as long as Q is identical to one of the Q_i.

It remains for us to discuss what happens to the curve if we change one of the weights, say β_k, and it turns out that we can use this parameter to modify the "flatness" of the curve at Q_k. Indeed, Schneider and Werner (1986) show that the derivative of P at $Q_k = P(t_k)$ is

$$P'(t_k) = \frac{\sum_{i=0,\, i\neq k}^{n} (-1)^{k+i+1} \frac{\beta_i}{t_k - t_i} (Q_k - Q_i)}{\beta_k}.$$

As the numerator, which determines the direction of the tangent at Q_k, does not depend on β_k, which in turn appears only in the denominator, it follows that β_k controls the length of the tangent, but not its direction. Therefore, decreasing β_k "flattens" the curve locally at Q_k, while increasing β_k has the effect of letting the curve bend more tightly at Q_k (see Fig. 2.c and Fig. 5). However, some limits on the possible values of β_k need to be respected, if we want to guarantee that the curve remains non-singular.

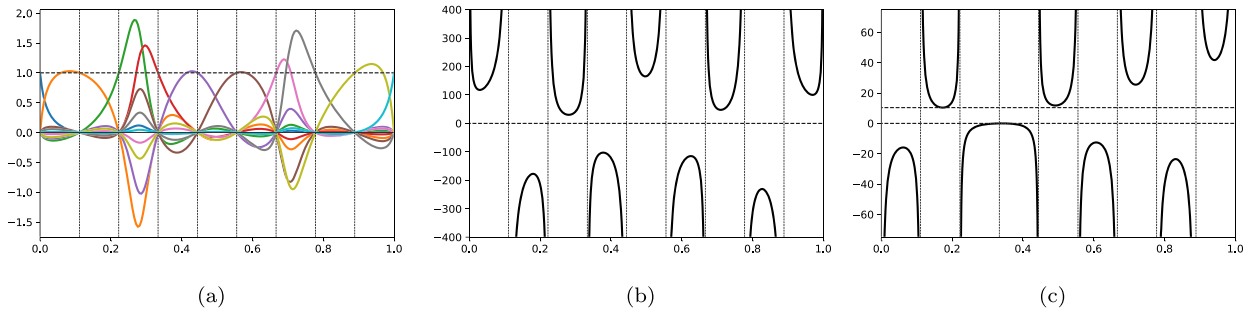

Fig. 4. Plots of (a) the basis functions $C_k(t)$ for $k = 0, \dots, n$ of a barycentric rational curve of degree $n = 9$ with equidistant nodes $t_i = i/n$ and weights $(\beta_0, \dots, \beta_n) = (1, 8, 3, 2, 5, 6, 2, 5, 8, 1)$, (b) the denominator $D(t)$, and (c) the function $S_k(t)$ for $k = 3$. The horizontal lines represent M_* and M^*.

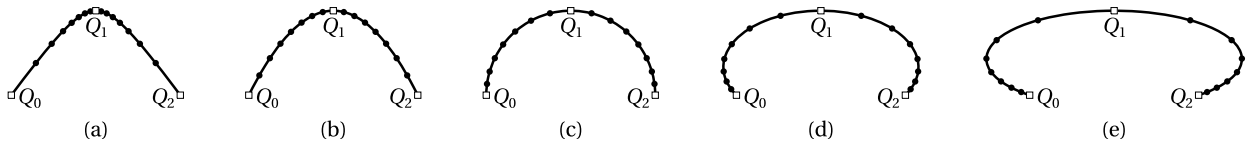

Fig. 5. The effect of changing the central weight of a quadratic rational curve P in barycentric form (3): (a) $\beta_1 = 4$; (b) $\beta_1 = 2$; (c) $\beta_1 = 1$; (d) $\beta_1 = 1/2$; (e) $\beta_1 = 1/4$. The direction of the derivative $P'(t_1)$ at Q_1 is fixed, but its length is inverse proportional to β_1. The dots visualize the curve points $P(i/16)$ for $i = 0, \dots, 16$.

Proposition 6. *Consider a non-singular barycentric rational curve (3) with nodes $0 = t_0 < t_1 < \cdots < t_n = 1$, interpolation points Q_i, and weights $\beta_i > 0$ and suppose we change the weight β_k for some $k \in \{0, \dots, n\}$ to some new value $\bar{\beta}_k$. Then the modified curve $\bar{P}$ remains non-singular as long as $\bar{\beta}_k \in (M_\star, M^\star)$, where*

$$M_\star = \max\{\dots, M_{k-2}, M_k, M_{k+2}, \dots\}, \qquad M^\star = \min\{\dots, M_{k-3}, M_{k-1}, M_{k+1}, M_{k+3}, \dots\},$$

with

$$M_{k+i} = \begin{cases} \max\{S_k(t) : t \in (t_{k+i+i_\star}, t_{k+i+i^\star})\}, & i \text{ even}, \\ \min\{S_k(t) : t \in (t_{k+i+i_\star}, t_{k+i+i^\star})\}, & i \text{ odd}, \end{cases} \qquad i_\star = \begin{cases} -1, & i \le 0, \\ 0, & i > 0, \end{cases} \quad i^\star = \begin{cases} 0, & i < 0, \\ 1, & i \ge 0, \end{cases} \tag{12}$$

and

$$S_k(t) = \sum_{i=0\, i\neq k}^{n} (-1)^{k+i+1} \frac{t - t_k}{t - t_i} \beta_i.$$

Proof. First recall from (5) that the denominator $D(t) = \sum_{i=0}^{n} (-1)^i \frac{\beta_i}{t - t_i}$ of a non-singular barycentric rational curve with positive weights β_i (see Fig. 4.b) satisfies

$$(-1)^n \ell(t) D(t) = \hat{z}(t) > 0, \qquad t \in [0, 1], \tag{13}$$

where $\ell(t) = \prod_{i=0}^{n} (t - t_i)$. Next observe that the denominator

$$\bar{D}(t) = (-1)^k \frac{\bar{\beta}_k}{t - t_k} + \sum_{i=0,\, i\neq k}^{n} (-1)^i \frac{\beta_i}{t - t_i}$$

of the modified curve $\bar{P}$ vanishes at $\bar{t}$, if and only if $\bar{\beta}_k = S_k(\bar{t})$. By the interpolation property of barycentric rational curves, it is clear that $\bar{t} \notin \{t_0, \dots, t_n\}$. Therefore, $\bar{P}$ is non-singular for $t \in [0, 1]$, as long as $\bar{\beta}_k$ is not in the image of $I = [0, 1] \setminus \{t_0, \dots, t_n\}$ under S_k. To better understand the behaviour of S_k, note that

$$S_k(t) = (-1)^{k+1} (t - t_k) D(t) + \beta_k$$

and assume that $t \in (t_j, t_{j+1})$ for some $j \in \{0, \dots, n-1\}$. Since $(-1)^{n-j} \ell(t)$ is clearly positive, it follows from (13) that $(-1)^j D(t)$ is positive too, with $\lim_{t \to t_j} (-1)^j D(t) = \lim_{t \to t_{j+1}} (-1)^j D(t) = +\infty$. Therefore, $S_k(t) - \beta_k$ is positive, if $j \ge k$ and $j + k$ is odd, or if $j < k$ and $j + k$ is even, and negative otherwise, converging to $+\infty$ or $-\infty$ as t approaches t_j or t_{j+1}, except at t_k, because $S_k(t_k) = 0$. Consequently, the image of (t_j, t_{j+1}) under S_k is

$$S_k[(t_j,t_{j+1})] = \begin{cases} [M_{j+1},+\infty), \\ (-\infty,M_{j+1}], \end{cases} \quad \text{if } j < k-1 \text{ and } j+k \text{ is } \begin{cases} \text{even}, \\ \text{odd}, \end{cases}$$

$$S_k[(t_j,t_{j+1})] = \begin{cases} [M_j,+\infty), \\ (-\infty,M_j], \end{cases} \quad \text{if } j \geq k+1 \text{ and } j+k \text{ is } \begin{cases} \text{odd}, \\ \text{even}, \end{cases}$$

and

$$S_k[(t_{k-1},t_{k+1})] = (-\infty,M_k],$$

for the M_j in (12) (see Fig. 4.c). Combining these images, we find that $S_k[I] = (-\infty,M_\star] \cup [M^\star,+\infty)$, which, together with the considerations above, shows that the stated condition for $\bar\beta_k$ guarantees $\bar P$ to be non-singular. □

Note that $M_\star$ in Proposition 6 is always non-negative, because $S_k(t_k) = 0$ and thus $M_\star \geq M_k \geq 0$, which is in line with our expectation that $\bar\beta_k$ should be positive, just like β_k, in order for $\bar P$ to be non-singular. In general, it does not seem feasible to determine the bounds $M_\star$ and $M^\star$ analytically, but they can be computed numerically by first finding the roots of S_k' over the relevant intervals with Newton's method, using, for example, the midpoint of the interval as initial value, and then evaluating S_k at these roots to get the M_j in (12).

Example 5. The derivative of the quadratic barycentric rational curve P with nodes $t_0 = 0$, $t_1 = 1/2$, $t_2 = 1$, interpolation points $Q_0 = (-1,0)$, $Q_1 = (0,1)$, $Q_2 = (1,0)$, and weights $\beta_0 = \beta_1 = \beta_2 = 1$ at t_1 is $P'(t_1) = (4,0)$ (see Fig. 5.c). Increasing the weight β_1 to 2 or 4 shortens the derivative by a factor of $1/2$ or $1/4$, respectively (see Fig. 5.a,b), while decreasing β_1 to $1/2$ or $1/4$ extends the derivative by a factor of 2 or 4, respectively (see Fig. 5.d,e). In this example, the curve is well-defined for all $\beta_1 > 0$. Instead, if we want to modify β_0, then we must ensure that $\beta_0 \in (0,9)$.

4. Point insertion and degree elevation

A common tool for increasing the flexibility of a rational Bézier curve is degree elevation, which can be used to represent a given curve of degree n as a curve of degree $n+1$ without changing its shape. This increases the number of control points and weights by one and hence gives the user more control to model the desired shape. The equivalent of degree elevation in the barycentric form simply amounts to adding an interpolation point $Q_\star = P(t_\star)$ for some $t_\star \in [0,1] \setminus \{t_0,\dots,t_n\}$, adapting the weights β_i, and computing the appropriate new weight for $Q_\star$.

Proposition 7. *Let $k \in \{0,\dots,n+1\}$ and $t_\star \in (t_{k-1},t_k)$, where $t_{-1} = 0$ and $t_{n+1} = 1$. The barycentric rational curve P of degree n in (3) with nodes t_i, interpolation points Q_i, and weights β_i can then be expressed alternatively as a barycentric rational curve $\breve P$ of degree $n+1$ with parameters*

$$\breve t_i = \begin{cases} t_i, \\ t_\star, \\ t_{i-1}, \end{cases} \qquad \breve Q_i = \begin{cases} Q_i, \\ Q_\star = P(t_\star), \\ Q_{i-1}, \end{cases} \qquad \breve\beta_i = \begin{cases} \frac{\beta_i}{t_\star - t_i}, \\ \sum_{i=0}^n (-1)^{n+k+i} \frac{\beta_i}{t_i - t_\star}, \\ \frac{\beta_{i-1}}{t_{i-1} - t_\star}, \end{cases} \quad \text{if } \begin{cases} i < k, \\ i = k, \\ i > k. \end{cases} \tag{14}$$

Proof. As in the proof of Proposition 5, we first use Proposition 4 to convert P to Bézier form and then conclude from Proposition 1 that the given weights satisfy $\beta_i = (-1)^{n+i} w_i \hat z(t_i)$, where w_i is defined in (4) and $\hat z(t) = \ell(t) \sum_{i=0}^n (-1)^n \frac{\beta_i}{t-t_i}$. Likewise, applying Proposition 1 to the nodes $\breve t_0,\dots,\breve t_{n+1}$, it follows that $\breve Q_i = P(\breve t_i)$, which simplifies to what is stated in (14), and that $\breve\beta_i = (-1)^{n+1+i} \breve w_i \hat z(\breve t_i)$, where $\breve w_i = \prod_{j=0,\, j\neq i}^{n+1} \frac{1}{\breve t_i - \breve t_j}$. If $i < k$, then this expression simplifies to

$$\breve\beta_i = (-1)^{n+1+i} \frac{1}{\breve t_i - \breve t_k} \prod_{j=0,\, j\neq i,k}^{n+1} \frac{1}{\breve t_i - \breve t_j} \hat z(\breve t_i) = (-1)^{n+1+i} \frac{1}{t_i - t_\star} \prod_{j=0,\, j\neq i}^{n} \frac{1}{t_i - t_j} \hat z(t_i) = \frac{\beta_i}{t_\star - t_i},$$

because $\breve t_i = t_i$ for $i < k$ and $\breve t_i = t_{i-1}$ for $i > k$, and similarly to

$$\breve\beta_i = (-1)^{n+1+i} \frac{1}{\breve t_i - \breve t_k} \prod_{j=0,\, j\neq i,k}^{n+1} \frac{1}{\breve t_i - \breve t_j} \hat z(\breve t_i) = (-1)^{n+1+i} \frac{1}{t_{i-1} - t_\star} \prod_{j=0,\, j\neq i}^{n} \frac{1}{t_{i-1} - t_j} \hat z(t_{i-1}) = \frac{\beta_{i-1}}{t_{i-1} - t_\star},$$

if $i > k$. For the remaining weight $\breve\beta_k$, note that $\ell(\breve t_k) = \prod_{j=0}^n (\breve t_k - t_j) = 1/\breve w_k$, hence

$$\breve\beta_k = (-1)^{n+1+k} \breve w_k \ell(\breve t_k) \sum_{i=0}^n (-1)^i \frac{\beta_i}{\breve t_k - t_i} = \sum_{i=0}^n (-1)^{n+k+i} \frac{\beta_i}{t_i - t_\star}. \quad \square$$

At this point, one may ask: what happens if we convert the barycentric rational curve $\breve{P}$ of degree $n+1$ with the parameters in (14) to Bézier form? But as $\breve{P}$ is just a different representation of the same curve P, its Bézier form must simply be the degree-elevated Bézier form of P. Indeed, since degree elevation does not change the denominator polynomial $\hat{z}$, this fact can also be observed by applying Proposition 1 to the degree-elevated Bézier form of P and noticing that this gives the parameters in (14).

Example 6. Adding the point $Q_\star = P(1/3)$ to the quadratic barycentric rational curve $\bar{P}$ from Example 4 (see Fig. 3.e), it follows from Proposition 7 that the quarter circle can be described as a cubic barycentric rational curve with nodes $\breve{t}_0 = 0$, $\breve{t}_1 = 1/3$, $\breve{t}_2 = 2/3$, $\breve{t}_3 = 1$, interpolation points $\breve{Q}_0 = (1,0)$, $\breve{Q}_1 = (12/13, 5/13)$, $\breve{Q}_2 = (3/5, 4/5)$, $\breve{Q}_3 = (0,1)$, and weights $\breve{\beta}_0 = 3$, $\breve{\beta}_1 = 13/2$, $\breve{\beta}_2 = 5$, $\breve{\beta}_3 = 3/2$ (see Fig. 3.f). Applying Proposition 4 to this curve, we find that its Bézier form is given by the control points $\breve{P}_0 = (1,0)$, $\breve{P}_1 = (1,1/2)$, $\breve{P}_2 = (2/3,1)$, $\breve{P}_3 = (0,1)$ and the weights $\breve{\alpha}_0 = 2/3$, $\breve{\alpha}_1 = 4/9$, $\breve{\alpha}_2 = 1/3$, $\breve{\alpha}_3 = 1/3$ (see Fig. 3.f), which is just the degree-elevated quadratic rational Bézier curve from Example 3 (see Fig. 3.d).

5. Performance of the barycentric form for curve evaluation

The classical way to evaluate a rational Bézier curve (1) at some parameter $t \in [0,1]$ is by applying the *de Casteljau algorithm* to the numerator and the denominator of $P(t)$ and dividing through, which has time complexity $O(n^2)$. The rational de Casteljau algorithm (Farin, 1983) provides a more robust, but less efficient alternative with the same time complexity. A recent paper by Woźny and Chudy (2020) presents a novel evaluation procedure for rational Bézier curves with a nice geometric interpretation. Like the de Casteljau algorithm, it is based on robust convex combinations, but it has a favourable linear time complexity. Yet another option is to use Proposition 1 to convert the curve into the barycentric form in (3) and to evaluate the latter. This can clearly be done in linear time, too, by first computing the sums in the numerator and the denominator and then dividing through (see Algorithm 1).

Algorithm 1 Evaluation of P using the barycentric rational form.

Input: nodes $t_0 \dots, t_n$, interpolation points $Q_0, \dots, Q_n$, and weights $\beta_0, \dots, \beta_n$ of P and parameter t
Output: $P(t)$

```
N := 0
D := 0
σ := 1
for i from 0 to n do
    d := t − t_i
    if d = 0 then
        return Q_i
    a := σ β_i / d
    N := N + a Q_i
    D := D + a
    σ := −σ
return N/D
```

To compare the efficiency of these three algorithms (classical de Casteljau, linear-time geometric, barycentric), we implemented them in C++ on an Ubuntu 20.04.2 LTS laptop with 1.8 GHz Intel Core i7-10510U processor and 16 GB RAM. The time complexities of the algorithms are confirmed by the plots in Fig. 6.a, which show the average running times for evaluating a rational Bézier curve of degree n with random control points $P_i \in [-1,1]^2$ and random weights $\alpha_i \in [0.01, 10]$ at 10^6 random parameters t for $n = 3, 5, 10, 20, \dots, 80$. Regardless of n, the evaluation in barycentric form is the fastest, even though the running time includes the time for pre-computing the interpolation points Q_i (with Woźny and Chudy's linear-time algorithm) and the weights β_i (with the polynomial de Casteljau algorithm) for equidistant nodes $t_i = i/n$ and Lagrange weights $w_i = (-1)^{n-i}\binom{n}{i} n^n/n!$ (Berrut and Trefethen, 2004). Compared to the 10^6 evaluations, this pre-computation is negligible, but for fewer evaluations it is not. This effect can be seen in Fig. 6.b, which reports the running times for evaluating a cubic rational Bézier curve at $M = 100, 200, \dots, 1000$ random parameters $t \in [0,1]$. While the linear-time algorithm is the fastest for small M, the pre-computation needed for the barycentric evaluation pays off for large M, with the break-even at about $M = 300$ evaluations.

While we use equidistant nodes in this comparison, we should point out that this may lead to numerical inaccuracies for $n \geq 50$, due to the large variance of the w_i, which carries over to the β_i. Instead, stable results can be obtained by using Chebyshev points of the second kind as nodes, that is, $t_i = (1 - \cos\frac{i\pi}{n})/2$, because the corresponding Lagrange weights satisfy $|w_0| = |w_n| = |w_i|/2$ for $i = 1, \dots, n-1$ (Berrut and Trefethen, 2004).

6. Conclusion

In this paper, we explored the use of barycentric rational curves in the context of shape design, and we studied their properties. Converting a given rational Bézier curve to barycentric form is simple and comes with several advantages. On the one hand, the barycentric form offers new tools for controlling the shape of the curve that are complementary to the

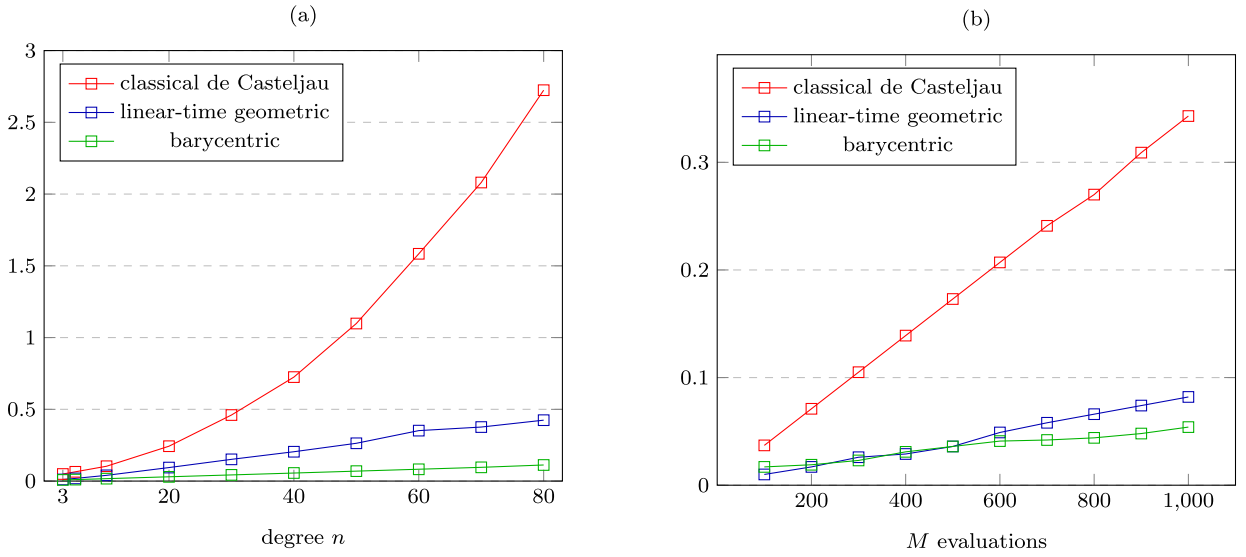

Fig. 6. Comparison of different algorithms for evaluating a rational Bézier curve: (a) running times (in seconds) for 10^6 evaluations of curves of different degree n; (b) running times (in milliseconds) for M evaluations of a curve of degree 3.

classical way of manipulating rational Bézier curves. As the barycentric form provides neither a convex hull, nor a vanishing diminishing property, these new tools may be less intuitive, but we believe that they are still useful, at least for "micro-editing". After a modification in the barycentric form, the curve can easily be transformed back into Bézier form. On the other hand, the barycentric form is very efficient to evaluate in linear time.

Analogously to rational Bézier curves, the barycentric rational curve P in (3) can be seen as the projection of the polynomial curve $\hat{P}$ that interpolates the homogeneous interpolation points $\hat{Q}_i = (z_i Q_i, z_i)$ at the nodes t_i, where $z_i = (-1)^{n+i}\beta_i/w_i$, into the $\hat{z} = 1$ plane. In this homogeneous setting, the proposed editing operations can be understood as follows: (1) "sliding" Q_k along P is equivalent to "sliding" $\hat{Q}_k$ along $\hat{P}$, and as the modification of t_k entails a change of the w_i, the β_i need to be updated for $i \neq k$ as in Proposition 5, so that the corresponding z_i and $\hat{Q}_i$ remain the same; (2) moving Q_k is like moving $\hat{Q}_k$ in the $\hat{z} = z_k$ plane; (3) modifying β_k is tantamount to displacing $\hat{Q}_k$ along the line through $\hat{Q}_k$ and the origin. The larger β_k, the further $\hat{Q}_k$ is from the origin, and the more the projected curve P bends at Q_k, very similarly to how increasing the weight α_i pulls P towards the control point P_k in the case of rational Bézier curves.

For the important class of non-singular rational curves, there is an interesting difference between the Bézier and the barycentric form. While the positivity of the α_i is *sufficient*, the positivity of the β_i is only *necessary* for the non-singularity of the curve. Consequently, the set of all Bézier curves with positive α_i does not contain all non-singular curves, while the set of all barycentric rational curves with positive β_i does, but also contains singular curves. In both cases, additional non-linear constraints are needed to fix this (cf. Proposition 6).

Another difference is that the barycentric form can describe curves that cannot be represented in Bézier form, at least not with the same degree. For example, a semi-circle can be modelled as a quadratic rational curve in barycentric form (see Fig. 5.c), but not in Bézier form without using control vectors, and likewise for a full circle as a quartic rational curve.

Declaration of competing interest

The authors certify that they have NO affiliations with or involvement in any organization or entity with any financial interest (such as honoraria; educational grants; participation in speakers' bureaus; membership, employment, consultancies, stock ownership, or other equity interest; and expert testimony or patent-licensing arrangements), or non-financial interest (such as personal or professional relationships, affiliations, knowledge or beliefs) in the subject matter or materials discussed in this manuscript.

Acknowledgements

This research is part of a project that has received funding from the European Union's Horizon 2020 research and innovation programme under the Marie Skłodowska-Curie grant agreement No 860843.

References

Antoulas, A.C., Anderson, B.D.O., 1986. On the scalar rational interpolation problem. IMA J. Math. Control Inf. 3, 61–88. https://doi.org/10.1093/imamci/3.2-3.61.

Berrut, J.P., 1988. Rational functions for guaranteed and experimentally well-conditioned global interpolation. Comput. Math. Appl. 15, 1–16. https://doi.org/10.1016/0898-1221(88)90067-3.
Berrut, J.P., Mittelmann, H.D., 1997. Lebesgue constant minimizing linear rational interpolation of continuous functions over the interval. Comput. Math. Appl. 33, 77–86. https://doi.org/10.1016/S0898-1221(97)00034-5.
Berrut, J.P., Trefethen, L.N., 2004. Barycentric Lagrange interpolation. SIAM Rev. 46, 501–517. https://doi.org/10.1137/S0036144502417715.
Bos, L., De Marchi, S., Hormann, K., Klein, G., 2012. On the Lebesgue constant of barycentric rational interpolation at equidistant nodes. Numer. Math. 121, 461–471. https://doi.org/10.1007/s00211-011-0442-8.
Dupuy, M., 1948. Le calcul numérique des fonctions par l'interpolation barycentrique. C. R. Hebd. Séances Acad. Sci. 226, 158–159.
Farin, G., 1983. Algorithms for rational Bézier curves. Comput. Aided Des. 15, 73–77. https://doi.org/10.1016/0010-4485(83)90171-9.
Farin, G., 2001. Curves and Surfaces for CAGD: A Practical Guide. The Morgan Kaufmann Series in Computer Graphics and Geometric Modeling, 5th ed. Morgan Kaufmann, San Francisco.
Farin, G., Worsey, A., 1991. Reparametrization and degree elevation of rational Bézier curves. In: Farin, G. (Ed.), NURBS for Curve and Surface Design. Society for Industrial and Applied Mathematics, Philadelphia, pp. 47–58.
Floater, M.S., Hormann, K., 2007. Barycentric rational interpolation with no poles and high rates of approximation. Numer. Math. 107, 315–331. https://doi.org/10.1007/s00211-007-0093-y.
Marco, A., Martínez, J.J., 2007. A fast and accurate algorithm for solving Bernstein–Vandermonde linear systems. Linear Algebra Appl. 422, 616–628. https://doi.org/10.1016/j.laa.2006.11.020.
Nakatsukasa, Y., Sète, O., Trefethen, L.N., 2018. The AAA algorithm for rational approximation. SIAM J. Sci. Comput. 40, A1494–A1522. https://doi.org/10.1137/16M1106122.
Patterson, R.R., 1985. Projective transformations of the parameter of a Bernstein–Bézier curve. ACM Trans. Graph. 4, 276–290. https://doi.org/10.1145/6116.6119.
Piegl, L., 1987. On the use of infinite control points in CAGD. Comput. Aided Geom. Des. 4, 155–166. https://doi.org/10.1016/0167-8396(87)90032-X.
Salzer, H.E., 1981. Rational interpolation using incomplete barycentric forms. Z. Angew. Math. Mech. 61, 161–164. https://doi.org/10.1002/zamm.19810610304.
Schneider, C., Werner, W., 1986. Some new aspects of rational interpolation. Math. Comput. 47, 285–299. https://doi.org/10.1090/S0025-5718-1986-0842136-8.
Taylor, W.J., 1945. Method of Lagrangian curvilinear interpolation. J. Res. Natl. Bur. Stand. 35, 151–155. https://doi.org/10.6028/jres.035.006.
Woźny, P., Chudy, F., 2020. Linear-time geometric algorithm for evaluating Bézier curves. Comput. Aided Des. 118, 102760. https://doi.org/10.1016/j.cad.2019.102760.